



Published in final edited form as:

*Eur Radiol.* 2008 November ; 18(11): 2466–2474. doi:10.1007/s00330-008-1019-5.

## Characterization of coronary atherosclerosis by dual-source computed tomography and HU-based color mapping: a pilot study

### **H Brodoefel,**

Department of Diagnostic Radiology, Eberhard-Karls-University, Hoppe-Seyler-Str. 3, 72076 Tübingen, Germany

Department of Radiology, Beth Israel Deaconess Medical Center, 330 Brookline Ave., 02215 Boston, MA, USA

### **A Reimann,**

Department of Diagnostic Radiology, Eberhard-Karls-University, Hoppe-Seyler-Str. 3, 72076 Tübingen, Germany

### **M Heuschmid,**

Department of Diagnostic Radiology, Eberhard-Karls-University, Hoppe-Seyler-Str. 3, 72076 Tübingen, Germany

### **I Tsiflikas,**

Department of Diagnostic Radiology, Eberhard-Karls-University, Hoppe-Seyler-Str. 3, 72076 Tübingen, Germany

### **A. F. Kopp,**

Department of Diagnostic Radiology, Eberhard-Karls-University, Hoppe-Seyler-Str. 3, 72076 Tübingen, Germany

### **S Schroeder,**

Department of Cardiology, Eberhard-Karls-University, Otfried-Müller-Str. 10, 72076 Tübingen, Germany

### **C. D. Claussen,**

Department of Diagnostic Radiology, Eberhard-Karls-University, Hoppe-Seyler-Str. 3, 72076 Tübingen, Germany

### **M. E. Clouse,** and

Department of Radiology, Beth Israel Deaconess Medical Center, 330 Brookline Ave., 02215 Boston, MA, USA

### **C Burgstahler**

Department of Cardiology, Eberhard-Karls-University, Otfried-Müller-Str. 10, 72076 Tübingen, Germany

## Abstract

To assess HU-based color mapping for characterization of coronary plaque, using intravascular ultrasound virtual histology (IVUS-VH) as a standard of reference. Dual-source computed

tomography and IVUS-VH were prospectively performed in 13 patients. In five lesions, HU thresholds of the color-coding software were calibrated to IVUS-VH. In a 15-lesion verification cohort, volumes of vessel, lumen and plaque or percentages of lipid, fibrous and calcified components were obtained through use of pre-set HU cut-offs as well as through purely visual adjustment of color maps. Calibrated HU ranges for fatty or fibrous plaque, lumen and calcification were -10-69, 70-158, 159-436 and 437+. Using these cut-offs, HU-based analysis achieved good agreement of plaque volume with IVUS (47.0 vs. 51.0 mm<sup>3</sup>). Visual segmentation led to significant overestimation of atheroma (61.6 vs. 51.0 mm<sup>3</sup>;  $P=0.04$ ). Correlation coefficients for volumes of vessel, lumen and plaque were 0.92, 0.87 and 0.83 with HU-based analysis or 0.92, 0.85 and 0.71 with visual evaluation. With both methods, correlation of percentage plaque composition was poor or insignificant. HU-based plaque analysis showed good reproducibility with intra-class correlation coefficients being 0.90 for plaque volume and 0.81, 0.94 or 0.98 for percentages of fatty, fibrous or calcified components. With use of optimized HU thresholds, color mapping allows for accurate and reproducible quantification of coronary plaque.

## Keywords

Dual-source computed tomography; HU-based plaque characterization; IVUS virtual histology

## Introduction

In pathological studies, rupture of the atherosclerotic coronary plaque has been related to specific compositional characteristics, one of which is the percentage amount of the lipid core [1-4]. Invasive coronary angiography (ICA) is the clinical standard technique to assess the extent of coronary artery disease. However, due to the phenomenon of coronary artery remodeling, advanced atherosclerosis may be found in non-stenotic coronary segments [5-7]. While grey-scale intravascular ultrasound (IVUS) is accepted as the standard of reference for detection and quantification of non-stenotic atheroma, it proves imprecise in the compositional characterization of plaque [8-10]. By comparison, spectrum analysis of IVUS-derived radiofrequency (RF), also known as IVUS virtual histology (IVUS-VH), enables differentiation of the four primary plaque components (necrotic core, fatty-fibrous, fibrous and calcified) [11-13].

In recent years, multi-slice computed tomography (MSCT) has emerged as a promising tool for non-invasive plaque characterization [14-20]. However, until now, its capacity to accurately quantify and characterize the non-calcified plaque has been restricted by limited temporal and spatial resolution. While Hounsfield units (HU) have been proven to be significantly different for the various plaque components, partial volume effects have restricted a prospective use of CT attenuation in the classification of atheroma [16, 20-24]. Therefore, in MSCT, segmentation of plaque was previously done by visual assessment and manual contouring.

Recently, a new dual-source CT system (DSCT) has been designed that is equipped with two tubes and corresponding detectors in a 90-degree geometry. It provides temporal resolution of approximately a quarter of its 330-ms gantry rotation time [25]. Likewise, dedicated software is now available that allows for more detailed investigation of non-calcified plaque through definition of a set of Hounsfield unit (HU) ranges and subsequent color mapping. This approach holds the promise of providing a more accurate or reproducible quantification of atheroma. Moreover, it may be used to investigate plaque composition just like IVUS-VH.

The potential benefit of color-coding software has not yet been assessed in comparison to spectrum analysis of IVUS-derived RF.

Hence, the aim of our feasibility study was to evaluate and optimize HU-based plaque-mapping techniques, using IVUS-VH as a standard of reference, and to compare findings with a visual assessment of atheroma.

## Materials and methods

### Study population

From September 2006 to March 2007 we studied 100 patients that were scheduled for conventional coronary angiography (ICA) due to suspected coronary artery disease (CAD) or suspected progression of known CAD. All DSCT studies were performed the day prior to ICA. Exclusion criteria were renal insufficiency (serum creatinine >1.5 mg/dl), hyperthyroidism (basal TSH <0.03  $\mu$ l/l in combination with elevated thyroid hormone levels in the peripheral blood), known allergic reaction against iodinated contrast media or inability to follow breath-hold commands.

In 13 of these patients (12 men and 1 woman;  $65 \pm 7$  years), IVUS was performed in at least one vessel to either evaluate the extent of in-stent restenosis (n=9) or to assess for plaque burden and composition in vessels without angiographic evidence of significant stenosis (n=4). Thereby, a total of 20 plaques was analyzed.

The study protocol was approved by the local ethics committee, and all patients gave informed consent for participation in the study.

### Grey-scale and IVUS-VH imaging protocol and data analysis

All IVUS studies were evaluated by a single, experienced observer blinded to the results of DSCT. IVUS-VH data were acquired with a dedicated IVUS-VH console (Volcano Corporation, Rancho Cordova, CA). A phased-array, 20-MHz, 3.2-F IVUS catheter (Eagle Eye, Volcano Corporation, Rancho Cordova, CA) was placed distally to the lesion of interest. Motorized pull-back was performed with a pull-back rate of 0.5 mm/s. The pull-back was stopped as soon as the IVUS catheter reached the guiding catheter. During the pull-back, a grey-scale IVUS was recorded, and raw RF data were captured at the top of the R wave. IVUS-VH data were transferred to an offline workstation and reconstructed using a commercial software tool (pcVH 2.1 software, Volcano Corporation, Rancho Cordova, CA). Thereby, the lumen and the media-adventitia interface were defined by automatic contour detection with manual editing on all individual frames. For every frame, morphometric parameters were expressed as cross-sectional area (CSA). Area of total plaque burden was defined as plaque plus media and calculated as  $Vessel_{area} - Lumen_{area}$ . Volumes of plaque burden per lesion, lumen and vessel were calculated according to Simpson's rule.

While for description of morphometric data plaque was defined as plaque plus media, the media was not included for calculation of compositional parameters. According to the radiofrequency signal processing, areas or volumes of the four characteristic plaque components were automatically determined for every recorded frame and for the entire imaged segment. Thereby, the necrotic core was displayed in red, the fatty-fibrous plaque in light green, the fibrous plaque in dark green and the calcified plaque in white color. For comparison with DSCT, IVUS-VH fatty-fibrous and necrotic core components were summed up as fatty plaque.

## CT coronary angiography

All CT examinations were performed on a dual-source CT system (Somatom Definition, Siemens Medical Solutions, Forchheim, Germany).

Before acquisition of the topogram, patients received a single dose of 0.8-mg glycerol trinitrate.

For contrast-enhanced examinations, vessel opacification was achieved through automated injection by a power injector (CT2™, Medtronic, Saarbrücken, Germany) of 80 ml iomeprol (Iomeron® 400, Altana, Konstanz, Germany) at a flow rate of 5 ml/s plus a 60 ml chaser bolus. Estimation of individual circulation time was based on the test bolus technique, using a 20-ml bolus and dynamic evaluation software (Dyn Eva™, Syngo®, Siemens, Forchheim, Germany).

Collimation was  $32 \times 0.6$  mm, slice acquisition  $64 \times 0.6$  mm using the z-flying focal spot technique, gantry rotation time 330 ms, pitch 0.20–0.43 adapted to heart rate, tube voltage 120 kV and maximum tube current 400 mAs per rotation. For dose reduction, prospective tube current modulation was applied. Thereby, at heart rates below 60 bpm, full tube current was applied from 60–70%, at 60–70 bpm from 50–80% and at heart rates above 70 bpm from 30 to 80% of the cardiac cycle. Given this scan protocol as well as the individual scan length and pitch of the CT exams, mean  $CTDI_{vol}$  was  $45.9 \pm 2.2$  mGy, mean dose-length product was  $549.1 \pm 35.6$  mGy  $\times$  cm, and mean effective dose was  $9.3 \pm 1.1$  mSv (CT-Exp, 1.6, G. Stamm and H.D. Nagel, Institute of Experimental Radiology, Hanover, Germany).

For data reconstruction, a single-segment reconstruction algorithm was applied that uses the data of a quarter rotation of both detectors for image reconstruction.

An initial reconstruction window was based on the results of a test series that was obtained in a transverse plane at the level of segment 2 (according to the AHA classification) and that displayed reconstruction window offsets by 5% of the entire cardiac cycle [26]. In case of motion artifacts in the initial reconstruction, further reconstructions were obtained in 5% increments of the cardiac cycle until all individual arteries could be visualized at optimal image quality.

Effective slice thickness was 0.75 mm with a reconstruction increment of 0.4 mm. Data sets were filtered with a medium-soft convolution kernel (B26f).

## DSCT image analysis

CT data were referred to an offline workstation (Leonardo, Siemens) and assessed using the Circulation III package (Siemens) and the Plaque Map software (Siemens) for vessel or plaque analysis. The software is based on curved multiplanar reconstructions (CPRs), and images are rendered along and orthogonally to the centre line of coronary arteries. Throughout the analysis, CPRs were displayed with a fixed window level and width of 200 and 800 HU. For additional orientation, thin-slab maximum-intensity-projections (MIP) and 3-D volume renderings were used.

Evaluation of plaque was performed according to the following multi-step protocol, illustrated in Fig. 1. In a first step, five plaques in five consecutive patients were studied to calibrate the HU thresholds of the Plaque Map software to IVUS or IVUS-VH (Fig. 2). Thereby, selection of target lesions in DSCT was interactively performed by reader 1 and 2 who were both de-blinded to the IVUS results of the specific patients. The subsequent adjustment of vessel or plaque volumes with calibration of HU thresholds was done by a de-blinded single reader 1. On CT CPRs, accurate matching of lesions to IVUS was ensured by

referring to lesion length and fiduciary markers (stents, side branches or characteristic calcifications) as defined in longitudinally reconstructed IVUS data. A maximal measurement-discrepancy of 5% was accepted with regard to length of segment. The semi-automatic vessel edge definition of the analysis software was employed and, whenever necessary, the vessel boundaries adapted to achieve a close match ( $\pm 5\%$ ) to the vessel volumes in IVUS. Subsequently, the threshold for the calcified plaque component was modified so that its volume equaled the results of IVUS-VH. The lower threshold for the fatty plaque component was always fixed to  $-10$  HU, and the cut-off for the vessel lumen was individually adjusted until the entire plaque burden matched to its volume in IVUS. For the individual adjustment of the cut-off between fatty and fibrous plaque, the relative proportion between the lipid and fibrous component was calculated in IVUS-VH and applied to DSCT through modification of the distinct HU threshold (Fig. 2). HU values for all thresholds were recorded, and the means of these values were used for further analysis of the verification group.

In step 2, analysis of another 15 plaque-containing segments (distributed in 8 patients) was performed by reader 1, who was blinded to the corresponding results in IVUS. As described above, matching of corresponding lesions was ensured by referring to lesion length and fiduciary markers. Again, a maximal measurement discrepancy of 5% was accepted with regard to length of the target lesion. Semi-automatic segmentation of vessel edge was applied and manually adjusted in case of obvious divergence from the outer vessel wall. Using the calibrated HU thresholds, volumes of vessel, lumen as well as low, medium and high density plaque components were automatically displayed by the Plaque Map software. Corresponding colors in the color-coding overlay were dark green for fatty plaque, light green for fibrous plaque and purple for calcified plaque. Yellow was used for vessel lumen.

In a third step, a visual assessment and segmentation of plaque was performed. To this end, the 15 plaques in the verification cohort were interactively analyzed by reader 3 and 4, who were blinded to IVUS and using the same segment markers and outer vessel edge definitions as reader 1. For each segment, HU cut-offs of the software were manipulated until the color maps most closely matched the visual aspect of plaque morphology.

In a fourth step, reader 1 was de-blinded to the IVUS results of the 15 plaques in the verification cohort and applied the same steps of matching as described for the calibration series. In addition, vessel attenuation was assessed in all of the 20 plaque-containing segments, taking the mean of three regions of interest measurements per lesion.

For assessment of inter-observer variability with HU-based plaque analysis, semi-automatic definition of the outer vessel boundaries was eventually repeated by reader 3, and plaque volumes in the verification cohort were reassessed by application of the calibrated HU cut-offs. For assessment of inter-observer variability with visual plaque evaluation, vessel edge definition and visual analysis were repeated by reader 2 and 4.

### Statistical analysis

Statistical analysis was performed with software (JMP version 6, SAS Institute, Cary, NC; GraphPad Prism version 4.00, San Diego, CA; SPSS version 15, Chicago, IL). A *P* value of less than 0.05 indicated statistical significance.

Continuous variables are expressed as mean  $\pm$  standard deviation, and comparisons between volumes and compositional percentages were performed using the t-test for paired observations. Bland-Altman analysis was used to display the systematic error and confidence interval (CI) between measurements, while the correlation between CT and IVUS variables is assessed in terms of the Pearson's correlation coefficient. Impact of heart

rate, body-mass index or percentage plaque calcification (as assessed in IVUS-VH) on the bias between plaque volume in IVUS and DSCT was tested by multivariate linear regression analysis and effect testing. Interaction between variables was checked by including multiplicative terms in the initial model. The impact of vessel attenuation on optimal HU cut-offs for lumen and fatty, fibrous or calcified plaque components is evaluated by linear regression. Interobserver reliability was assessed by calculating 2-way random single-measure intraclass correlation coefficients (ICC).

## Results

Plaque-containing segments were unequivocally identified on CPRs through fiducial markers and segment length. In the verification cohort, distribution of lesions was the following: 1 lesion in the left main artery; 7 lesions in the left anterior descending (n=4 segment 6; n=2 in segment 7; n=1 in segment 8), 5 lesions in the circumflex (n=5 segment 11) and 2 in the right coronary artery (n=1 segment 1; n=1 segment 2).

Results of the quantitative vessel or plaque analysis are provided in Table 1. While a HU-based evaluation achieved good concordance of volumes, visual segmentation was associated with significant overestimation of plaque burden ( $P=0.04$ ) or underestimation of lumen ( $P=0.003$ ; Fig. 3). According to multivariate regression, heart rate, body-mass-index and percentage plaque calcification had no significant effect on the bias between plaque volumes in IVUS or visual and HU-based analysis in DSCT.

In terms of percentage plaque composition, visual assessment resulted in significant overestimation of the lipid ( $P=0.0001$ ) or underestimation of the fibrous plaque component ( $P=0.004$ ). Again, good agreement was noted for a HU-based plaque characterization (Table 2).

HU-based color coding achieved good inter-modality correlation for the entire plaque burden ( $r=0.83$ ), whereas correlation was somewhat weaker for a visual assessment of atheroma ( $r=0.71$ ; Table 1; Fig. 4). Except for visual assessment of calcification, correlation regarding the percentages of plaque composition turned out to be poor and insignificant with both methods of CT plaque analysis (Table 2).

According to the initial calibration experiment, thresholds used for the HU-based analysis of the verification series were  $-10-69$  for low density,  $70-158$  for medium density,  $159-436$  for lumen and  $437-$  for high density plaque. The corresponding mean HU ranges resulting from visual adjustment of color maps were  $-16-88$ ,  $89-172$  and  $471-$ . Mean cut-offs as determined from IVUS-VH calibration of all 20 lesions were  $-10-66$ ,  $67-153$ ,  $154-446$  and  $447-$ .

In a linear regression considering the effect of vessel attenuation on IVUS calibrated cut-offs for lumen and plaque components, a considerable correlation was found for the optimal threshold of calcium ( $r=0.50$ ). A significant but very small association was observed between vessel attenuation and the IVUS correlated cut-off for lumen ( $r=0.29$ ; Fig. 5).

Intraclass correlation coefficients for volumes of vessel, lumen, plaque and low, medium or high attenuation components were 0.91, 0.98, 0.90, 0.81, 0.94 and 0.98 with HU-based lesion analysis. Corresponding coefficients with visual evaluation were 0.92, 0.90, 0.82, 0.56, 0.68 and 0.98. In the 15-lesion verification cohort, there was no significant difference between the vessel volumes as obtained through blinded semi-automatic versus deblinded IVUS adjusted contour drawing ( $115.6 \pm 53.6$  vs.  $123.3 \pm 57.1$  mm<sup>3</sup>;  $P=0.09$ ).

Imaging examples are provided in Fig. 6.

## Discussion

Until now, the analysis of CT attenuation within a coronary plaque was limited by motion and partial volume artifacts. Hence, CT density values have not primarily been employed in quantification and characterization of atheroma, but have only been retrospectively measured in visually detected plaque components [16, 20–23].

In this study, we have assessed the benefit of increased temporal resolution and color-coding software in terms of coronary plaque characterization. Our primary findings are threefold: First, when compared to purely visual analysis, prospective use of CT attenuation provides better correlation of total plaque volume with IVUS. With both forms of analysis, percentage plaque composition is not significantly correlated with IVUS-VH. Finally, optimal HU ranges as observed in our study partly differ from suggested thresholds in previous investigations, and, moreover, show a significant association with vessel enhancement.

In our head-to-head comparison between visual and HU-based color coding, the former was not only associated with inferior correlation, but also led to considerable overestimation of total plaque volume. Indeed, results of our HU-based analysis also compare favorably to previous studies that use visual or manual segmentation for volumetric plaque quantification. While Achenbach and Leber et al. found a comparable degree of correlation with IVUS, both studies report significant biases for overall plaque volume [14, 15]. Considerable inter-modality discrepancy has, likewise, been established in a variety of studies quantifying plaque in terms of cross-sectional area [17, 18, 27].

A strong asset to HU-based evaluation is a greatly improved inter-observer reproducibility. Inter-observer variability has previously been described as a major limitation to visual plaque segmentation [15]. In our study, it was particularly high for volumes of lipid or fibrous plaque components. Using pre-defined HU cut-offs, plaque analysis becomes independent of display settings, and interreader variability will merely correlate with modifications in the semiautomatic definition of vessel boundaries.

While results of our pilot study were promising in terms of plaque quantification, assessment of percentage plaque composition turned out to be inaccurate. Despite good concordance of mean percentages with HU-based color mapping, correlation of compositional data with IVUS-VH was only poor or insignificant. An obvious explanation is the possibility of inaccurate vessel segmentation and inclusion of pericardial fat in the CT analysis of plaque. Another important reason lies with the as yet limited spatial resolution of DSCT, which is certainly insufficient to dissect the complexity of plaque morphology. As frequently been demonstrated for fatty and fibrous plaque components, partial volume effects result in a considerable overlap of density values [16, 20–23]. Moreover, all of our plaques displayed a relatively homogeneous composition. With mean percentages of 30.3, 55.9 and 13.8 for lipid, fibrous and calcified components, none of the plaques in our pilot study fulfilled the criterion of vulnerability, notably a lipid core of more than 40% [28]. Given such limited distribution of compositional data, further analysis is needed to explore the degree of correlation in collectives with larger heterogeneity as well as the potential of HU-based color coding to ultimately identify the vulnerable atheroma.

In previous studies, CT density values of non-calcified plaque have frequently been obtained from ex vivo autopsy material or from ROI measurements in tissue that was visually correlated to hypoechoic and hyperechoic areas in IVUS. We assumed that assessment of average attenuation would be more accurate in vivo and when obtained from plaque tissue, the compositional percentages of which had previously been matched or calibrated to IVUS-VH. In doing so, we found markedly higher HU ranges for fibrous plaque than earlier

reported in the literature [16, 20, 29]. Interestingly, our results are in agreement with more recent comparisons of MSCT to IVUS [21–23]. Arguably, variations in spatial resolution of scanners, radiation dose application and maximal luminal attenuation exert a considerable effect on thresholds for such tissues that are in close proximity and have similar CT densities to the enhancing vessel lumen. This concept is in accordance with the considerable correlation we found between vessel attenuation and optimal cut-off for calcified plaque. A significant yet weak association was noted between vessel enhancement and the lower HU threshold for lumen. Our findings imply that whenever vessel attenuation varies, fixed HU cut-offs may produce inaccurate results for calcified plaque. Notably, the correlation of the calcified plaque component with IVUS-VH was considerably better when calcification was assessed visually rather than by use of HU cut-offs. On the other hand, for quantification of non-calcified plaque, use of pre-defined HU thresholds appears promising over a wide variability of vessel enhancement and turns out to be more accurate than visual evaluation. Ultimately, we suggest using our calibrated cutoffs as default values for HU-based plaque analysis. Adjustment of thresholds to discrepant contrast protocols or scanner technology is, however, mandatory, as is the verification of our results in larger series.

The small number of observations is an obvious limitation to our pilot study. This is especially true with regard to the power of non-significant statistical findings, notably the rejection of heart rate, body-mass index or calcification as predictors of precision in CT plaque quantification. Since IVUS was performed in the proximal lesion only, vessel diameters were relatively large. The same was true for average plaque volumes. Reproducibility of our results in more distal segments and with smaller plaques needs confirmation in further studies. The potential to use two X-ray tubes with different voltages to thus further characterize plaque composition has not been exploited.

In summary, initial experience suggests that a HU-based analysis provides accurate quantification of coronary plaque. When compared to visual segmentation of atheroma, the use of pre-defined thresholds results in superior precision and reproducibility. While in our pilot series percentage plaque composition showed no correlation to IVUS-VH, we provide optimized HU cut-offs that may guide larger studies on non-invasive plaque characterization. The good reproducibility of volumetric data makes HU-based color coding an attractive tool for longitudinal studies on plaque stabilization.

## References

1. Falk E, Shah PK, Fuster V. Coronary plaque disruption. *Circulation*. 1995; 92:657–671. [PubMed: 7634481]
2. Kragel AH, Reddy SG, Wittes JT, Roberts WC. Morphometric analysis of the composition of atherosclerotic plaques in the four major epicardial arteries in acute myocardial infarction and in sudden coronary death. *Circulation*. 1989; 80:1747–1756. [PubMed: 2598434]
3. Libby P. Molecular bases of the acute coronary syndromes. *Circulation*. 1995; 91:2844–2850. [PubMed: 7758192]
4. Naghavi M, Libby P, Falk E, et al. From vulnerable plaque to vulnerable patient: a call for new definitions and risk assessment strategies: Part I. *Circulation*. 2003; 108:1664–1672. [PubMed: 14530185]
5. Mintz GS, Painter JA, Pichard AD, et al. Atherosclerosis in angiographically “normal” coronary artery reference segments: an intravascular ultrasound study with clinical correlations. *J Am Coll Cardiol*. 1995; 25:1479–1485. [PubMed: 7759694]
6. Nissen SE, Gurley JC, Grines CL, et al. Intravascular ultrasound assessment of lumen size and wall morphology in normal subjects and patients with coronary artery disease. *Circulation*. 1991; 84:1087–1099. [PubMed: 1884441]



7. Topol EJ, Nissen SE. Our preoccupation with coronary luminology. The dissociation between clinical and angiographic findings in ischemic heart disease. *Circulation*. 1995; 92:2333–2342. [PubMed: 7554219]
8. Nishimura RA, Edwards WD, Warnes CA, et al. Intravascular ultrasound imaging: in vitro validation and pathologic correlation. *J Am Coll Cardiol*. 1990; 16:145–154. [PubMed: 2193046]
9. Potkin BN, Bartorelli AL, Gessert JM, et al. Coronary artery imaging with intravascular high-frequency ultrasound. *Circulation*. 1990; 81:1575–1585. [PubMed: 2184946]
10. Yock PG, Linker DT. Intravascular ultrasound. Looking below the surface of vascular disease. *Circulation*. 1990; 81:1715–1718. [PubMed: 2184950]
11. Moore MP, Spencer T, Salter DM, et al. Characterisation of coronary atherosclerotic morphology by spectral analysis of radiofrequency signal: in vitro intravascular ultrasound study with histological and radiological validation. *Heart*. 1998; 79:459–467. [PubMed: 9659192]
12. Nair A, Kuban BD, Tuzcu EM, Schoenhagen P, Nissen SE, Vince DG. Coronary plaque classification with intravascular ultrasound radiofrequency data analysis. *Circulation*. 2002; 106:2200–2206. [PubMed: 12390948]
13. Nasu K, Tsuchikane E, Katoh O, et al. Accuracy of in vivo coronary plaque morphology assessment: a validation study of in vivo virtual histology compared with in vitro histopathology. *J Am Coll Cardiol*. 2006; 47:2405–2412. [PubMed: 16781367]
14. Achenbach S, Moselewski F, Ropers D, et al. Detection of calcified and noncalcified coronary atherosclerotic plaque by contrast-enhanced, submillimeter multidetector spiral computed tomography: a segment-based comparison with intravascular ultrasound. *Circulation*. 2004; 109:14–17. [PubMed: 14691045]
15. Leber AW, Becker A, Knez A, et al. Accuracy of 64-slice computed tomography to classify and quantify plaque volumes in the proximal coronary system: a comparative study using intravascular ultrasound. *J Am Coll Cardiol*. 2006; 47:672–677. [PubMed: 16458154]
16. Leber AW, Knez A, Becker A, et al. Accuracy of multidetector spiral computed tomography in identifying and differentiating the composition of coronary atherosclerotic plaques: a comparative study with intracoronary ultrasound. *J Am Coll Cardiol*. 2004; 43:1241–1247. [PubMed: 15063437]
17. Leber AW, Knez A, von Ziegler F, et al. Quantification of obstructive and nonobstructive coronary lesions by 64-slice computed tomography: a comparative study with quantitative coronary angiography and intravascular ultrasound. *J Am Coll Cardiol*. 2005; 46:147–154. [PubMed: 15992649]
18. Moselewski F, Ropers D, Pohle K, et al. Comparison of measurement of cross-sectional coronary atherosclerotic plaque and vessel areas by 16-slice multidetector computed tomography versus intravascular ultrasound. *Am J Cardiol*. 2004; 94:1294–1297. [PubMed: 15541250]
19. Schoenhagen P, Tuzcu EM, Stillman AE, et al. Non-invasive assessment of plaque morphology and remodeling in mildly stenotic coronary segments: comparison of 16-slice computed tomography and intravascular ultrasound. *Coron Artery Dis*. 2003; 14:459–462. [PubMed: 12966267]
20. Schroeder S, Kopp AF, Baumbach A, et al. Noninvasive detection and evaluation of atherosclerotic coronary plaques with multislice computed tomography. *J Am Coll Cardiol*. 2001; 37:1430–1435. [PubMed: 11300457]
21. Carrascosa PM, Capunay CM, Garcia-Merletti P, Carrascosa J, Garcia MF. Characterization of coronary atherosclerotic plaques by multidetector computed tomography. *Am J Cardiol*. 2006; 97:598–602. [PubMed: 16490420]
22. Iriart X, Brunot S, Coste P, et al. Early characterization of atherosclerotic coronary plaques with multidetector computed tomography in patients with acute coronary syndrome: a comparative study with intravascular ultrasound. *Eur Radiol*. 2007
23. Pohle K, Achenbach S, Macneill B, et al. Characterization of non-calcified coronary atherosclerotic plaque by multi-detector row CT: comparison to IVUS. *Atherosclerosis*. 2007; 190:174–180. [PubMed: 16494883]

24. Schmid M, Pflederer T, Jang IK, et al. Relationship between degree of remodeling and CT attenuation of plaque in coronary atherosclerotic lesions: An in-vivo analysis by multidetector computed tomography. *Atherosclerosis*. 2007
25. Flohr TG, McCollough CH, Bruder H, et al. First performance evaluation of a dual-source CT (DSCT) system. *Eur Radiol*. 2006; 16:256–268. [PubMed: 16341833]
26. Bashore TM, Bates ER, Berger PB, et al. American College of Cardiology/Society for Cardiac Angiography and Interventions Clinical Expert Consensus Document on cardiac catheterization laboratory standards. A report of the American College of Cardiology Task Force on Clinical Expert Consensus Documents. *J Am Coll Cardiol*. 2001; 37:2170–2214. [PubMed: 11419904]
27. Hara T, Yamada S, Hayashi T, et al. Accuracy of nonstenotic coronary atherosclerosis assessment by multi-detector computed tomography. *Circ J*. 2007; 71:911–914. [PubMed: 17526989]
28. Davies MJ, Richardson PD, Woolf N, Katz DR, Mann J. Risk of thrombosis in human atherosclerotic plaques: role of extracellular lipid, macrophage, and smooth muscle cell content. *Br Heart J*. 1993; 69:377–381. [PubMed: 8518056]
29. Becker CR, Nikolaou K, Muders M, et al. Ex vivo coronary atherosclerotic plaque characterization with multi-detector-row CT. *Eur Radiol*. 2003; 13:2094–2098. [PubMed: 12692681]

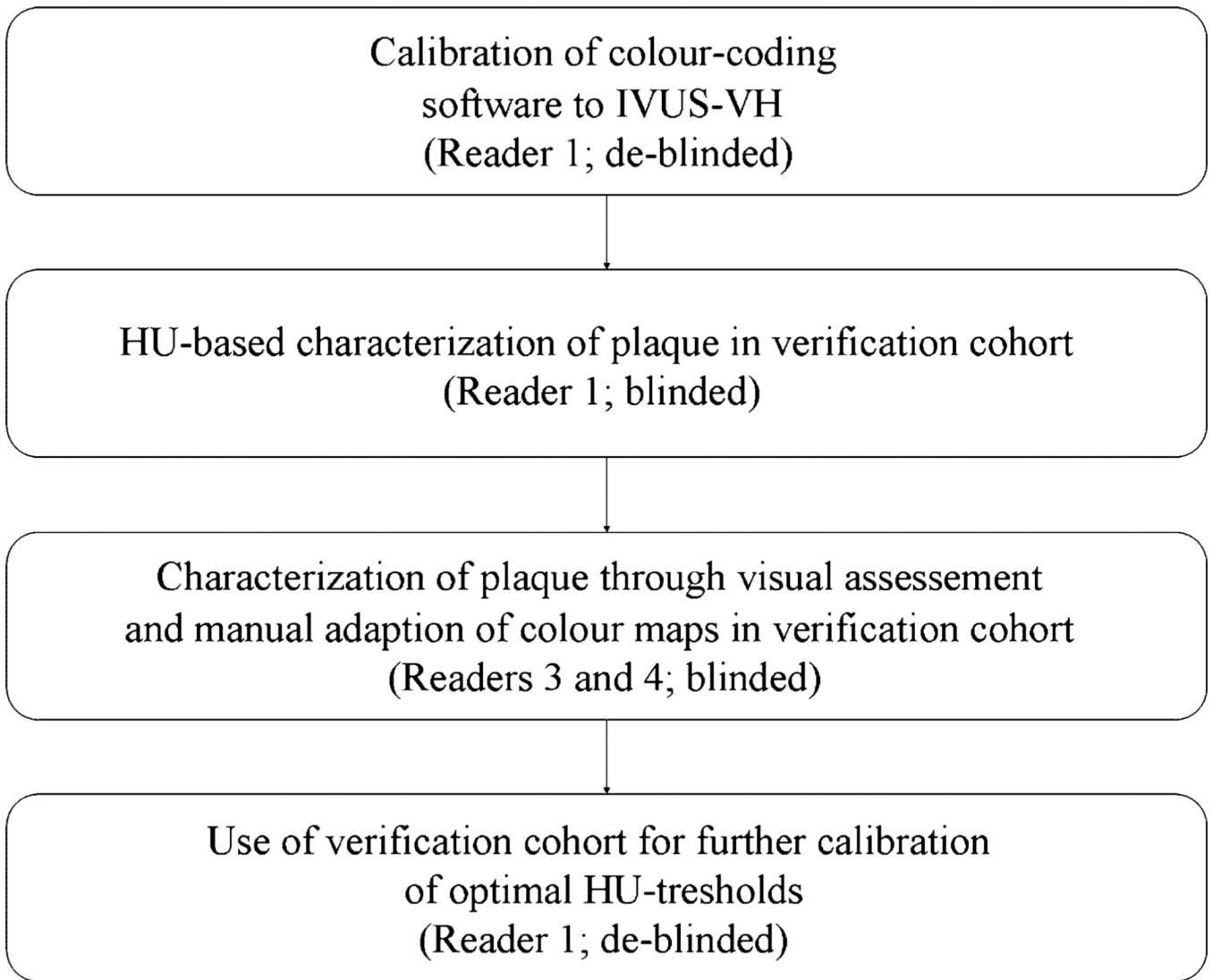


**Fig. 1.**  
Schematic description of the data analysis procedure

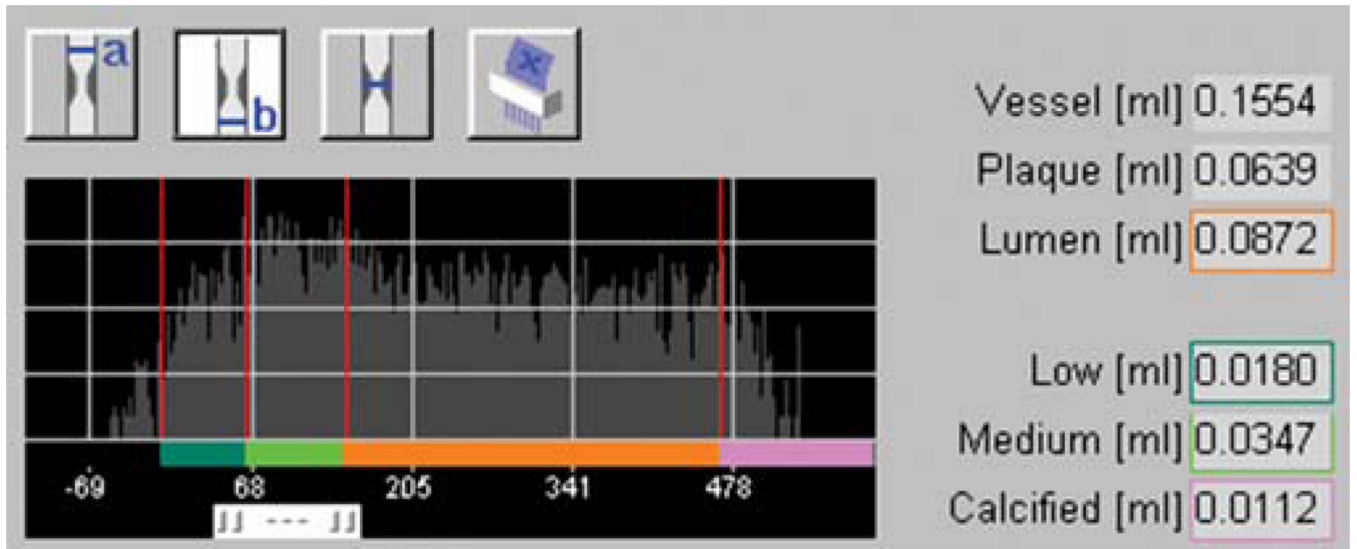


**Fig. 2.** Illustration of plaque analysis tool. HU distribution in plaque and vessel is shown with thresholds for fatty (dark green), fibrous (light green) and calcified atheroma (purple). Modification of thresholds results in change of plaque volume and volumes of its various components

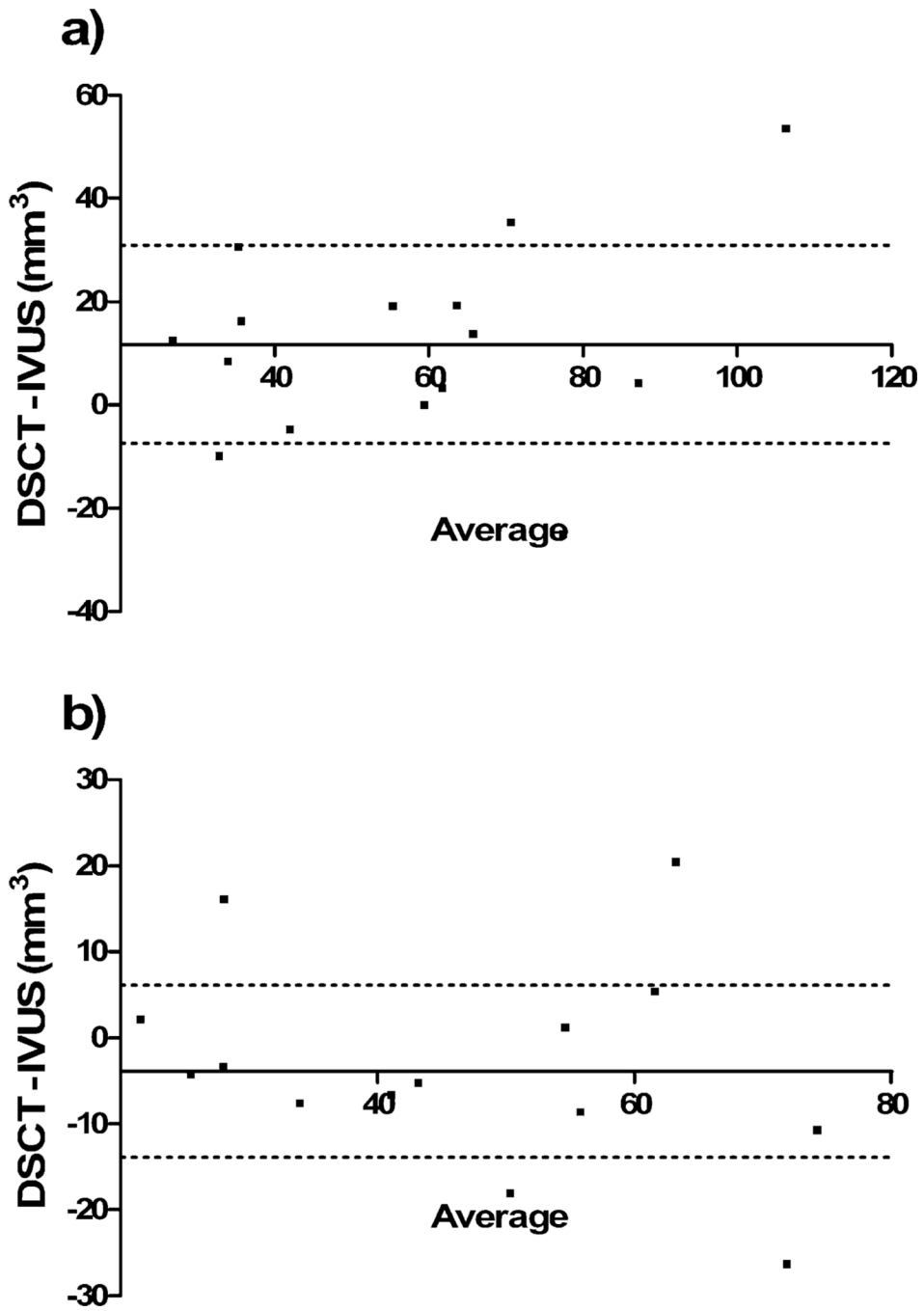


**Fig. 3.** Bland-Altman analysis comparing total plaque volumes as obtained with DSCT and IVUS. Data are shown for visual adjustment of color maps to plaque (**a**) and evaluation based on HU thresholds (**b**). The X axis denotes the average of DSCT and IVUS; the point of intersection with the Y axis indicates the bias of DSCT. Dotted lines show 1 standard deviation of the bias

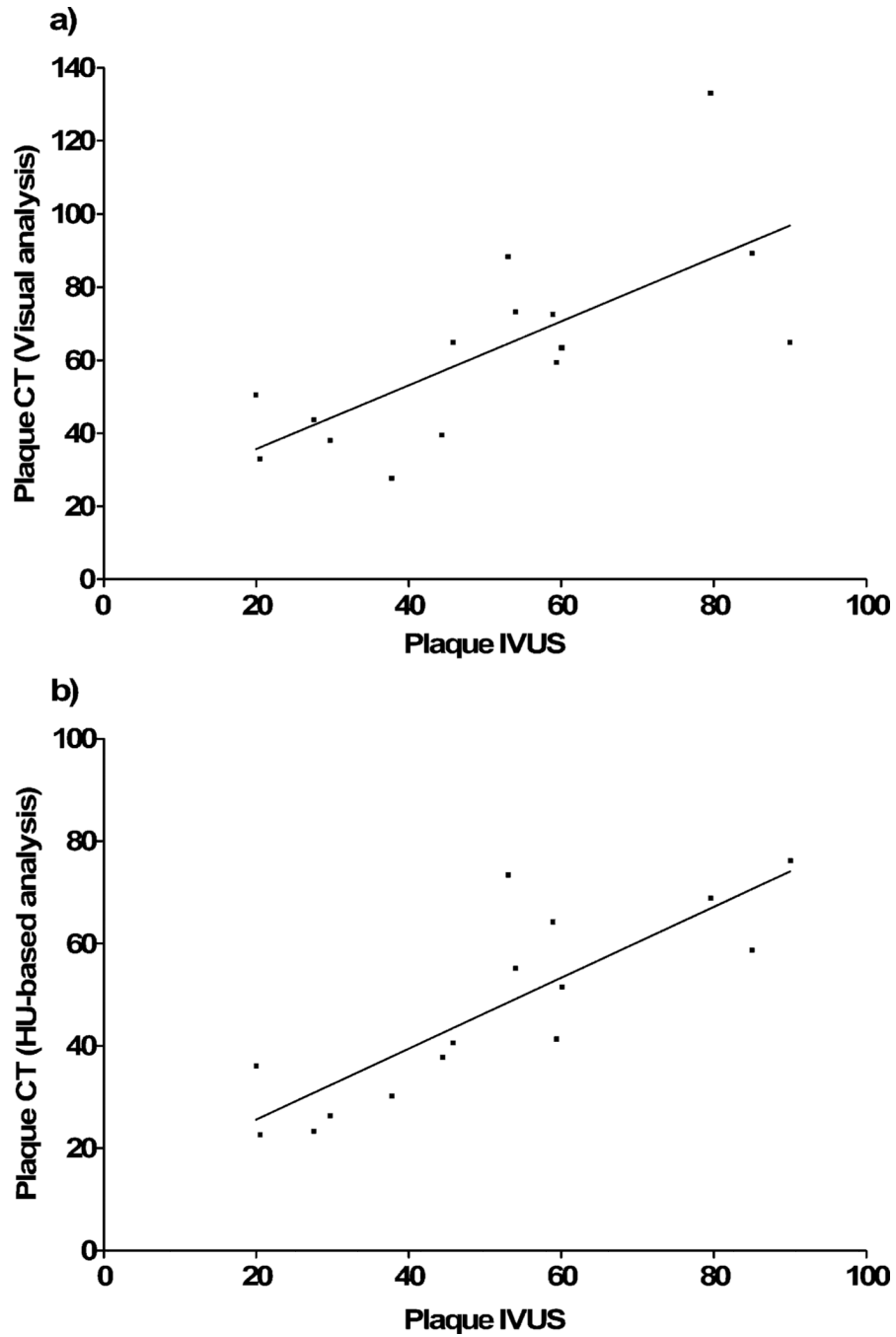


**Fig. 4.** Correlation of total plaque volumes in DSCT with IVUS. Data are shown for visual adjustment of color maps to plaque (a) and evaluation based on HU thresholds (b)

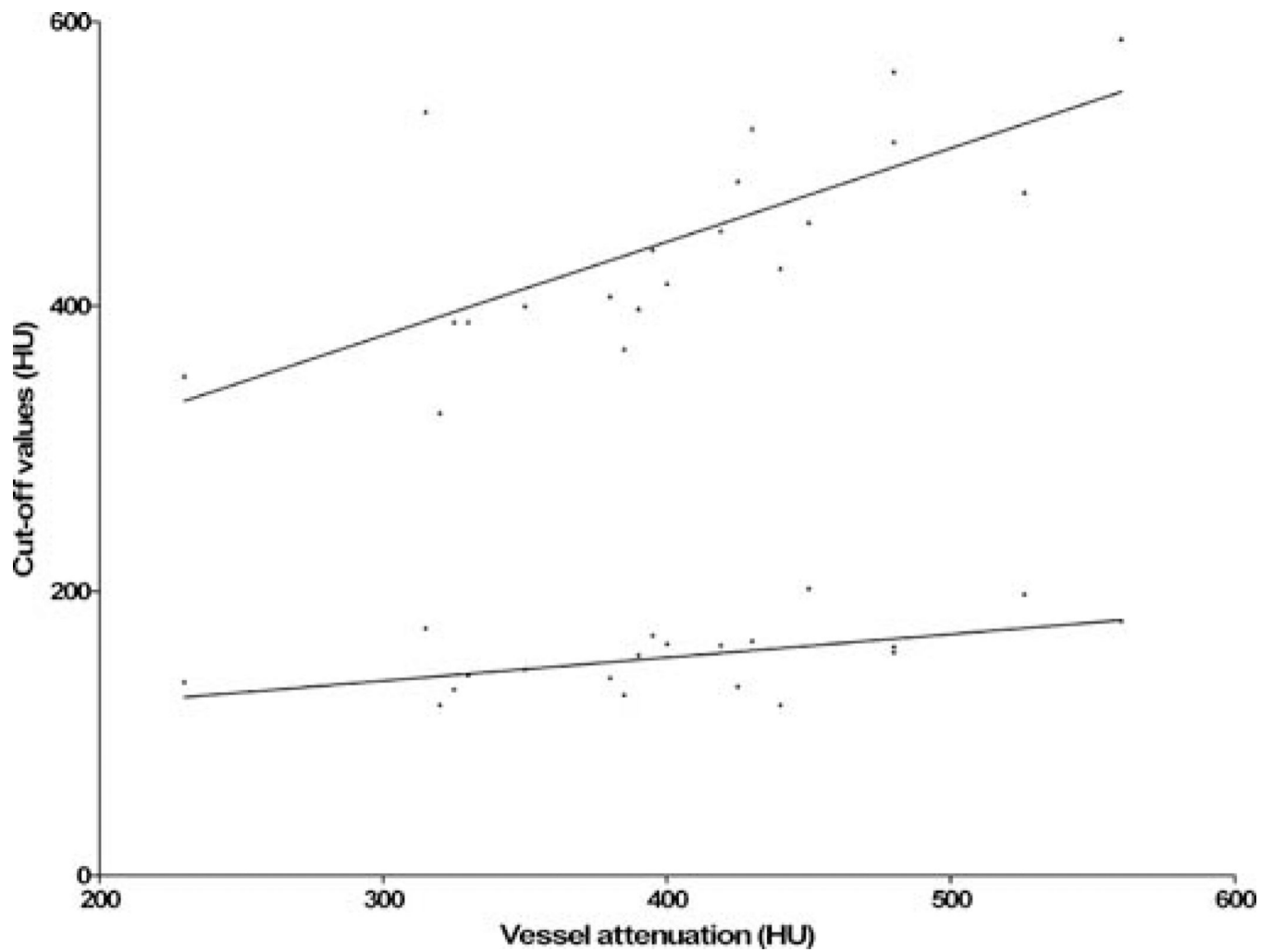


**Fig. 5.** Linear regression plot of optimal IVUS calibrated lower and upper HU cut-offs for lumen against attenuation in the distinct vessel segment

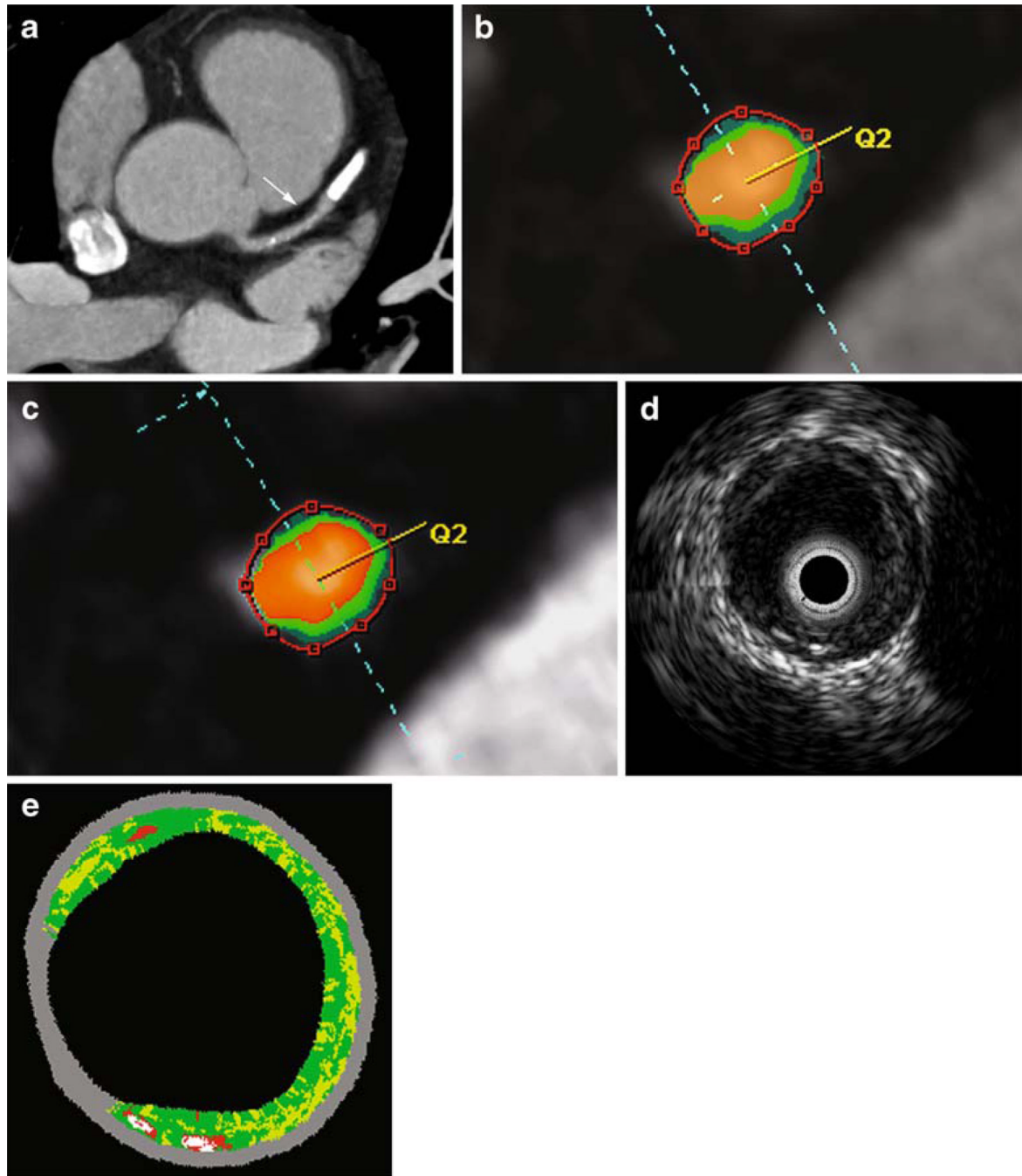


**Fig. 6.** Virtual plaque histology in DSCT and IVUS. In an axial MIP, the arrow indicates a non-calcified plaque in segment 6 of the LAD (a). Cross-sectional images of the vessel with color coding are presented for visual adjustment of the maps (b) or HU-based segmentation (c) as well as for grey-scale IVUS (d) and IVUS-VH (e). For IVUS-VH, red indicates necrotic core, light green the fatty-fibrous, dark green the fibrous and white the calcified plaque. In this lesion, total plaque volumes with visual CT evaluation, HU-based analysis or IVUS were 66.6 mm<sup>3</sup>, 55.8 mm<sup>3</sup> or 53.1 mm<sup>3</sup> respectively



**Table 1**

Volumes of vessel, lumen and plaque with visual adjustment of color maps versus HU-based analysis

	DSCT		IVUS
	Visual analysis	HU-based analysis	
Vessel (mm <sup>3</sup> )	115.6±53.6; <i>P</i> =0.29 -5.5; CI -17 to 5 <i>r</i> =0.92	115.6±53.6; <i>P</i> =0.29 -5.5; CI -17 to 5 <i>r</i> =0.92	121.1±50.9
Lumen (mm <sup>3</sup> )	53.5±24.8; <i>P</i> =0.003 -16.6; CI -28 to -8 <i>r</i> =0.85	67.4±29.9; <i>P</i> =0.32 -2.7; CI -14 to 5 <i>r</i> =0.87	70.1±34.0
Plaque burden (mm <sup>3</sup> )	61.6±26.6; <i>P</i> =0.04 10.6; CI 0 to 21 <i>r</i> =0.71	47.0±18.3; <i>P</i> =0.22 -4; CI -11 to 3 <i>r</i> =0.83	51.0±22.1

*P*-values refer to comparison with IVUS. The deviation of means is expressed by bias and confidence interval (CI); the degree of correlation with IVUS is given as the Pearson's correlation coefficient

**Table 2**

Percentages of fatty, fibrous or calcified plaque components with visual adjustment of color maps versus HU-based analysis

	DSCT		IVUS-VH
	Visual analysis	HU-based analysis	
Fatty component (%)	46.0±8.0; <i>P</i> =0.0001 15.2; CI 23 to 10 <i>r</i> =0.12	33.9±6.8; <i>P</i> =0.49 3.7; CI -3 to 5 <i>r</i> =0.32	30.3±5.1
Fibrous component (%)	44.7±9.3; <i>P</i> =0.004 -10.0; CI -4 to -18 <i>r</i> =0.31	50.1±11.4; <i>P</i> =0.09 -5.6; CI -12 to 1 <i>r</i> =0.43	55.9±11.7
Calcified component (%)	9.3±9.7; <i>P</i> =0.07 -4.5; CI -9 to 0.3 <i>r</i> =0.56	16.0±13.6; <i>P</i> =0.75 2.2; CI -7 to 10 <i>r</i> =0.11	13.8±8.2

*P*-values refer to comparison with IVUS. The deviation of means is expressed by bias and confidence interval (CI); the degree of correlation with IVUS-VH is given as the Pearson's correlation coefficient